# A novel experimental approach for assessment of impacts due to magnetic fields from submarine HVDC cable systems on benthic infauna

Joanna **RZEMPOŁUCH**, Amber **JONES**, Kevin **GODDARD,** Sunny **CHAUDHARY,** Neil **PALMER,** William **WU,** George **CALLENDER**, Justin **DIX**, Jasmin A **GODBOLD,** Martin **SOLAN,** Paul **LEWIN**; University of Southampton, (United Kingdom), jr9g20@soton.ac.uk, amber.jones@soton.ac.uk, kfg1@soton.ac.uk, sc.chaudhary@soton.ac.uk, n.l.palmer@soton.ac.uk, william.wu@soton.ac.uk, g.m.callender@soton.ac.uk, j.k.dix@soton.ac.uk, j.a.godbold@soton.ac.uk, m.solan@soton.ac.uk, pll@soton.ac.uk

Muhammad **SHABAN**, Hayley **TRIPP**, David **RENEW**; National Grid, (United Kingdom), muhammad.shaban@nationalgrid.com, hayley.tripp@nationalgrid.com, david.renew@nationalgrid.com

## *ABSTRACT*

*In this work, an experimental design for the evaluation of impacts of magnetic fields from HVDC cables on benthic animals is presented. Unlike previous studies, the vector orientation of the field and the spatial distribution are non-uniform, representing the magnetic fields from an HVDC system more accurately. The setup is designed using numerical models and tested to show that no additional stresses are imposed in the experiment and that the device produces the magnetic fields predicted by the models. Biological techniques quantifying behavioural changes and stresses are described to present a complete approach for the experimental design.*

## *KEYWORDS*

Magnetic fields, HVDC cable systems, Experiments, Benthic infauna.

## INTRODUCTION

In recent years, HVDC cable systems have been increasingly used both as interconnectors and in offshore wind farms located further from the shore. As many marine organisms are capable of magnetoreception and use geomagnetic field as a navigational cue, there have been rising concerns regarding the impacts of HVDC systems on the behaviour and physiology of marine life [1]. Benthic animals (i.e. animals living in or on the seabed, typically within the top 0.1 m) will be in closer proximity to the cable, as cables are usually buried in the sediment (burial depth of approx. 1m). This spatial relationship increases the potential of exposure to higher magnetic field strength.

Most of the EMF (electromagnetic field) related research focused on understanding of mechanisms behind the electro- and magnetoreception. It is known that the mechanisms of EMF detection and the parameters which are detected vary depending on the species [2],[3]. For instance, sea turtles, salmon, and lobster were shown to have the ability to detect both the intensity of the magnetic field and the information about the magnetic field vector direction [4], [5]. Some animals are believed to rely on the direction of the horizontal component of the magnetic field only, whilst others also partially rely on the inclination of the field for directional navigation [5]. This highlights the importance of the consideration of vector orientation of the field and its spatial distribution in experiments relating to submarine cables.

In most publications aiming to reproduce the EMFs from submarine cables, an arrangement of Helmholtz coils placed outside the tanks is used [6-16]. Helmholtz coils are often used as they do not require high currents to produce a magnitude of the field comparable to that typical for HV cables. A schematic of Helmholtz coils and a magnetic field associated with them is presented in Fig. 1.

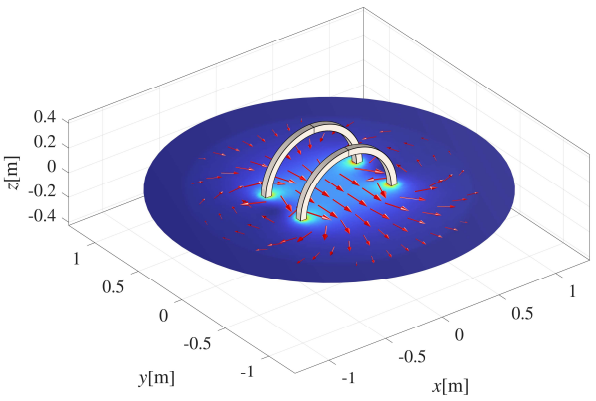


**Fig. 1: A schematic of Helmholtz coils arrangement used in reviewed experiments, reproduced using a model from** [17]**. The magnetic field inside the coils is unidirectional and uniform.**

Several publications focus solely on reproducing the magnetic field intensity. In this approach, two Helmholtz coils connected in series are placed on two sides of the tank to create a relatively uniform field within the tank [6], [9], [11], [13], [15], or alternatively, a single Helmholtz coil is used with the tank placed inside it [7], [8]. While this approach can be useful for experiments on animals which remain stationary, a uniform distribution does not represent the magnetic field accurately if the spatial change in field or the magnetic field vector orientation is what the animals respond to.

Other publications introduce a magnetic field gradient by placing two Helmholtz coils that only partially cover the tank to recreate a magnetic field decrease in the rest of the tank [10], [14], [16] . Although introducing a magnetic field spatial variance is more representative of a real cable scenario, the direction of the magnetic field vector in this arrangement changes by 180° as the animals move between the part of the tank covered by the Helmholtz coils to the uncovered part. The magnetic field norm rapidly drops and then increases around the edge of the coil. Thus, even though the overall magnetic field norm decreases, it does so in a way unrepresentative of a real-life scenario as it decreases faster than a field from an HV cable, and it does so with a fluctuation close to the edge of the coil.

In [12], an alternative method including a magnetic field gradient was used. None of the tanks were placed inside

the two Helmholtz system described earlier. Instead, the tanks were placed outside on both sides of the system. In this way, the direction of the magnetic field vector does not change while the magnetic field norm drops with the distance which is preferable to the methods outlined in [10], [14], [16] .

In [7], besides the Helmholtz coil setup, an arrangement of four electric solenoid magnets was used to create magnetic field norms of 2.8 mT and 40 mT. The distribution of the magnetic fields created this way is very localised and unrepresentative of the conditions close to the cable.

These commonly employed approaches create mostly unidirectional, and often uniform fields, as opposed to an HVDC cable which has components of the magnetic field in both horizontal and vertical directions.

## Magnetic fields typical for HVDC systems

HVDC cables most commonly appear in a bipole or monopole configuration. The magnetic field, from a monopole cable can be assumed to be

$$B = \frac{\mu_0 I}{2\pi R}\,\hat{\boldsymbol{\phi}}, \qquad (1)$$

where $I$ is the current, $R$ is the radial distance from the centre of the cable and $\mu_0$ is the permeability of the vacuum. Equation (1) is expressed in cylindrical coordinates centred on the conductor axis, where $\hat{\boldsymbol{\phi}}$ is the azimuthal angle unit vector. In the bipole case, the magnetic fields from individual cables add in between the cables and cancel everywhere else leading to a reduced magnetic field far from the cable, as shown in Table 1. The typical distribution of the magnetic field and the associated vector orientation of the field is presented in Fig. 2. The materials were assumed to be non-magnetic, and the cable geometry was taken from [18].

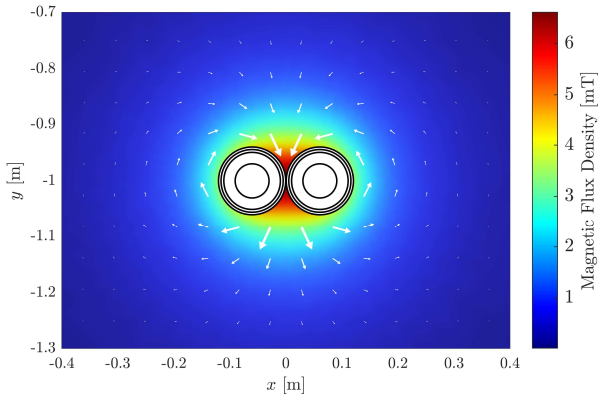


**Fig. 2: Magnetic field and vector orientation of an HVDC bipole cable system, calculated for a current of 1000 A and no core separation.**

| Distance Along *y*-axis (m) | Magnetic Field (mT) |
|---|---|
| 0 | 6.6 |
| 0.1 | 1.77 |
| 0.5 | 0.095 |
| 0.7 | 0.049 |
| 1 | 0.024 |

**Table 1: Magnetic field values vs distance computed for the cable in Fig.2. Distance of 0 m indicates the middle of the cable system.**

In this work, an alternative experimental setup is designed and tested to address the limitations of the previous approaches. The setup produces a non-uniform field with a vector orientation that resembles a HVDC bipole cable system, the most used type of HVDC cable systems.

## SETUP REQUIREMENTS

In this section, the requirements of the setup used for testing on benthic animals are introduced. The experiment design includes multiple cores (experimental aquaria) for storing animals that are located at different distances on either side of a device producing magnetic fields. In this setup, SCAMPI (Synthetic Cable for the Assessment of Marine Power Impacts) is used to produce the magnetic fields; the design of SCAMPI is introduced in the subsequent section. A schematic of the experiment is presented in Figs. 3 and 4. The device is placed in a main tank where it is fully covered in water. The water in the main tank is used for cooling the cores and SCAMPI to a temperature that is representative of the temperature the animals experienced during collection. Thermocouples are placed in the water and connected to PicoLog so that the temperature of the tank can be monitored in real time. The individual aquaria are continuously supplied with aerates seawater.

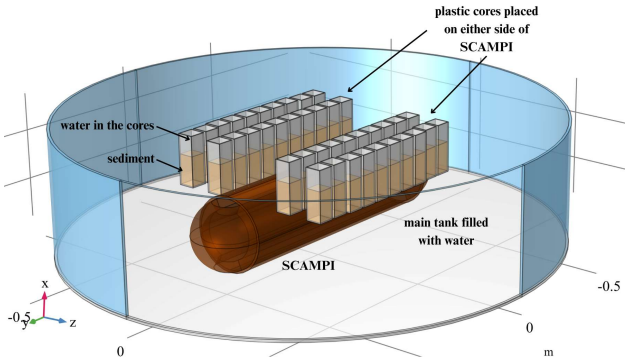


**Fig. 3: A schematic indicative of the experimental setup used in experiments on benthic fauna.**

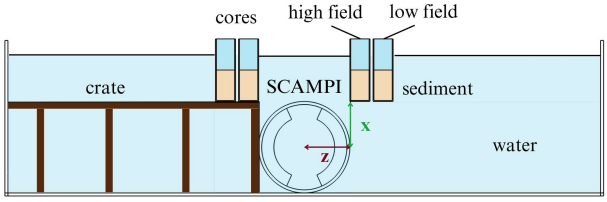


**Fig. 4: A 2D slice representing the setup for experiments on benthic animals.**

## EXPERIMENTAL DESIGN

In this section, we present the design of SCAMPI through numerical models constructed in COMSOL Multiphysics. The device has been developed to recreate non-uniform magnetic fields typical for HVDC cable systems. The proposed solution includes a wire wrapped in multiple turns enclosed in a polyacetal enclosure. Multiple turns were used to create an enhanced magnetic field of a distribution similar to a HV cable. To ensure that SCAMPI produces magnetic fields equivalent to those from an HV cable, the prototypes of SCAMPI were developed through multiple

numerical models, including both 2D and 3D electromagnetic models. The final device has a diameter of 30 cm and a length of 1.25 m. Previously SCAMPI was used in a case study presented in [19]. However, the design and testing of the device were not disclosed.

## 2D modelling

The magnetic field produced by SCAMPI using the 2D model is presented in Fig. 5. The setup was designed in a way that will allow for fields of up to ~ 2 mT in cores located 10 cm from the device's surface, similarly to the values indicated in Table 1. Various cable sizes and coil turns, as well as the separation of the rows, were considered to arrive at the final design. SCAMPI was intended to be of similar size to a submarine cable whilst producing similar fields to it. The device in the model is supplied with a current of 130 A, to recreate fields similar to an HVDC bipole, the current flows in opposite directions on two sides of SCAMPI through multiple turns. A bigger separation between the two conductor rows would result in higher magnetic field outside of the device. However, the size was intended to be small enough so that it does not introduce constraints to future experiments with different requirements.

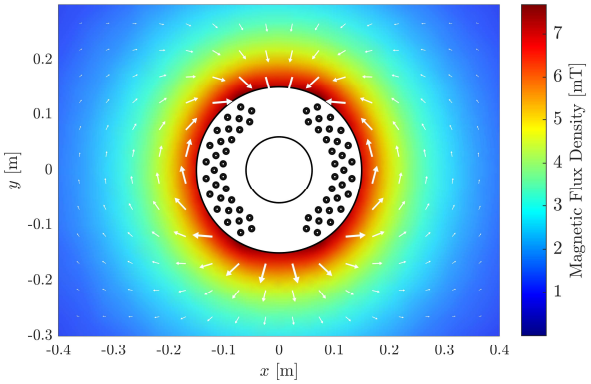


**Fig. 5: A 2D model of SCAMPI, magnetic fields are plotted for a current of 130 A.**

The 2D model does not consider the effects associated with the fact that SCAMPI has a finite length of around 1.2 m as the model extends to infinity in the *z*-direction. At close distances to the device, the 2D model is an accurate representation of the field since the distance from SCAMPI is small compared to its length. However, at distances comparable to SCAMPI's length and further, the effects of the edges of SCAMPI become more pronounced, altering the magnitude and spatial distribution of the field.

## 3D modelling

To address the limitations of the 2D model, a 3D model of SCAMPI was developed to model the field further from the device. The model was reduced to an octant to reduce computational power. 'Perfect Magnetic Conductor' was applied to the boundary marked as blue, and a 'Symmetry' boundary condition was applied to the boundaries marked as green in Fig. 6. The remaining external boundaries were set to be magnetically insulating. The individual conductors were modelled using the 'Coil' function.

Figs. 7 and 8 present the magnetic field produced by the proposed setup. Due to the limited length of the device the position of the cores located on the edges was adjusted to obtain a less than 6.5% variation of the mean magnetic field in the sediment volume across all aquaria.

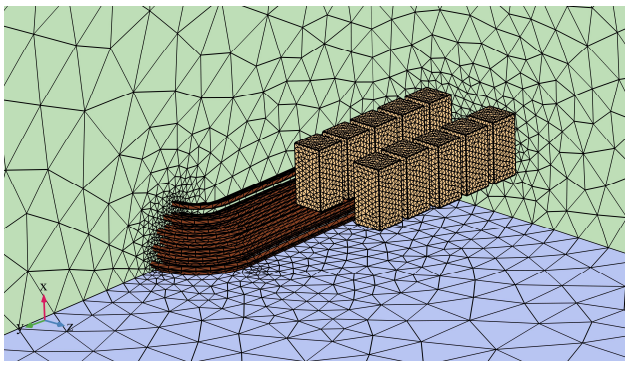

**Fig. 6: Geometry and mesh of the 3D model reduced to an octant.**

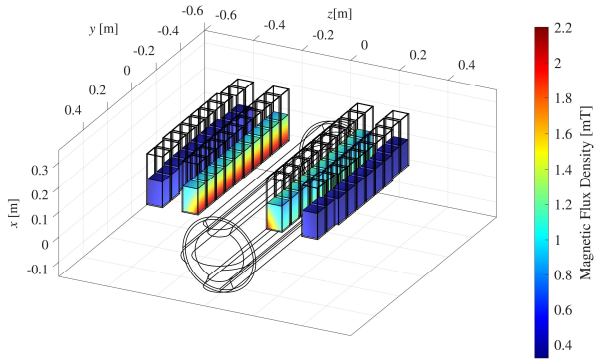


**Fig. 7: Magnetic field produced in cores using a current of 60 A.**

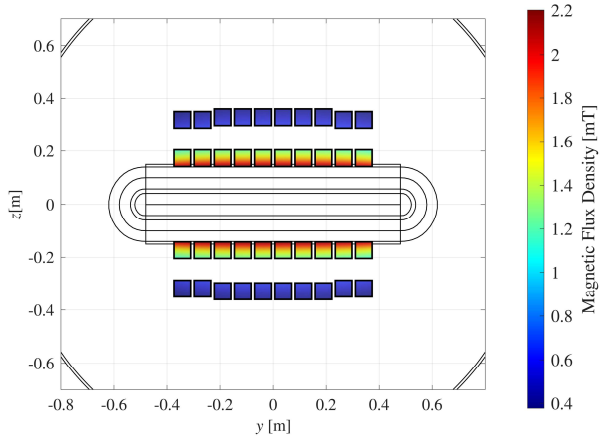


**Fig. 8: A surface plot of the magnetic field produced in the cores with animals plotted at the bottom of the cores for a current of 60 A.**

## Mechanical support

The mechanical support was developed to hold the conductors in place without the conductors touching and overheating. It consists of six Delrin plates connected using three parallel bars. The mechanical enclosure was developed in Solid Works. The model was then laser-cut, and the cable was wound through the mechanical support. The sketch of the final design made in Solid Works is included in Fig. 9. The assembled device is shown in Fig 10.

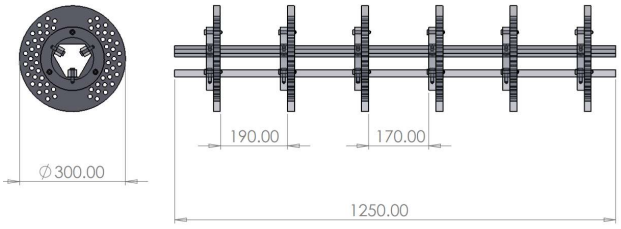


**Fig. 9: A SolidWorks sketch of the mechanical support, the dimensions are given in [mm].**

**Fig. 10: SCAMPI after assembly.**

## TESTING

The device has been tested to ensure that no additional stresses are imposed in the experiments, i.e. the temperature and noise, and that the magnetic fields agree with ones predicted by the numerical models. The results of performed testing are presented in this section.

### Supply

As SCAMPI requires a constant current of up to 130 A to operate, a DC supply rated for up to 200 A is used. The current during testing is measured using a clamp meter connected to PicoLog to collect the information about the current remotely and ensure that the magnetic field produced by the setup is kept constant, as the magnetic field is proportional to the current. Thermocouples are placed in the tank to ensure a stable temperature.

### Acoustic

The noise from the device was measured at six different locations using a hydrophone. The sample rate used for recording was set to 4000 Hz, and each recording lasted 10 seconds. The gain of RESON EC6081 mk2 preamplifier was set to be 30 dB, and the B & K type 8105 spherical hydrophone with a receiving sensitivity of -205 dB re 1V/µPa was used. The highest background noise level recorded was 117.89 dB re 1 µPa (with the device switched off), which was mostly due to the mains noise as indicated by the frequencies of the recorded signals. The measurements were then repeated with the device switched on. The highest value recorded was 0.4% above the background noise, with no obvious pattern change in spectrograms. Thus, the noise generated by the device was considered negligible.

### Thermal

The temperature in the tank was measured overnight to test the efficiency of the chiller used in the experiment. The experimental design includes a temperature measurement using the thermocouples connected to PicoLog Cloud enabling remote tracking of the temperature. The average temperature for SCAMPI energised with 90 A over 24 hours was 12.7 ºC with the maximum and minimum variation from the mean of ± 0.4 ºC.

### Electromagnetic

The magnetic field was experimentally validated using the Physics Toolbox app. Measurements were taken in the middle of SCAMPI in 5 cm increments in the middle of the device extending to 0.7 m, the current of 123 A was used. The resulting magnetic field norm was compared against the 3D results, as shown in Fig. 11. The measurements were adjusted for the background geomagnetic field measured at the location. The differences observed are likely due to the uncertainty regarding the exact position of the sensor and its spatial resolution. As demonstrated by Fig. 11, the magnetic field agrees with the predicted simulation values, the average percentage error with respect to the numerical solution was 5%.

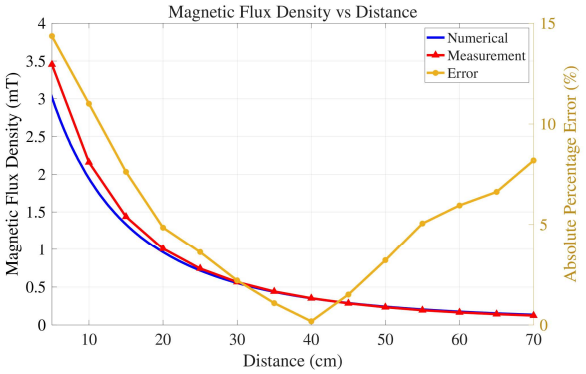


**Fig. 11: Validation of the predicted magnetic field magnitude.**

## OTHER EMF CONSIDERATIONS

As analysed in [19], in addition to magnetic fields, there can be electric fields induced in the seabed due to the water movement above the HVDC cable system. This effect has not been included in the proposed setup and modifying the setup to include this effect would be challenging as it would need to involve a set of electrodes in each core. However, an example setup which models this effect has been presented in [19]. The electric fields associated with the motionally induced electric fields are in the order of magnitude of $10^{-2}$ mV/m.

## BIOLOGICAL METHODS

The methods outlined here are broadly applicable across sediment invertebrates, including echinoderms, polychaetes, and gastropods. Within this framework, organisms can be assessed for changes in ecologically significant processes such as sediment reworking through bioturbation, porewater exchange via bioirrigation, and physiological responses including oxygen consumption. The integration of SCAMPI with acrylic cores provides a platform that can be tailored to the behavioural ecology of different taxa. Aquarium dimensions and sediment depth can be adjusted to mimic natural habitat conditions, accommodating species ranging from small, surface-oriented deposit feeders to large, deep-burrowing or tube-building species.

### Bioturbation

Within this setup, sediment reworking can be quantified using fluorescent luminophores applied to the sediment

surface utilising a method known as fluorescent sediment particle imagery [20]. These tracers allow high-resolution measurements of bioturbation activity, including maximum reworking depth ( $^{f}$-SPI$_{Lmax}$), mean and median reworking depths ( $^{f}$-SPI$_{Lmean,}$ $^{f}$-SPI$_{Lmedian}$), and changes in surface boundary roughness (SBR). Such measurements capture both the intensity and spatial structure of sediment disturbance, providing a mechanistic link between electromagnetic field exposure and alterations in benthic behaviour (Fig. 12).

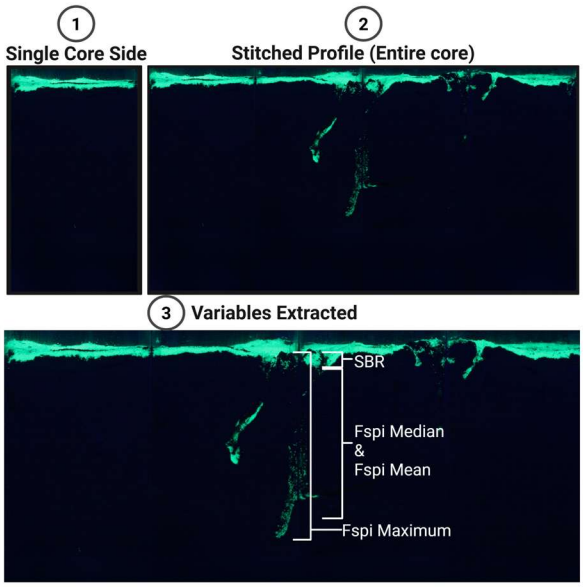


**Fig. 12: Imaging of fSPI process. Individual UV images of square acrylic cores containing fluorescent luminophores are stitched to create a full sediment profile. The processed image illustrates how reworking metrics (SBR, $^{f}$-SPI$_{Lmax}$, $^{f}$-SPI$_{Lmedian}$ and $^{f}$-SPI$_{Lmean}$) are associated. Created in BioRender. Jones, A. (2025) https://BioRender.com/ecfz7cw**

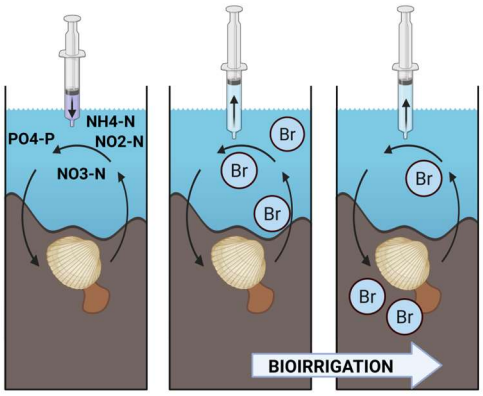


**Fig. 13: Method of bioirrigation process, illustrating the addition of a bromide tracer solution to sediment cores. Two porewater samples were collected: one immediately following tracer addition and a second after an 8-hour incubation period. Created in BioRender. Jones, A. (2025) https://BioRender.com/a1l5x0t**

## Bioirrigation and Nutrient Dynamics

The use of cores allows quantification of ventilatory behaviour and solute exchange across the sediment water interface in response to EMF exposure [21]. Tracer additions (bromide) resolve bioirrigation rates, while nutrient analyses of overlying water track nitrogen and phosphorus fluxes [22] (Fig. 13). This experimental design enables these measurements to be made alongside bioturbation, providing an integrated framework for assessing benthic functioning under EMF conditions.

## Physiology

To assess physiological responses to electromagnetic field (EMF) exposure, closed-loop respirometry offers a sensitive method for measuring oxygen consumption as a proxy for metabolic rate [23]. This approach can provide valuable insights into organismal energy expenditure and potential stress responses linked to EMF conditions. Within this framework, oxygen concentrations can be continuously logged using optical sensors adapted into a lid to seal the core systems [24]. Incorporating a small internal recirculating pump within each core is recommended to ensure homogeneous mixing and minimize boundary layer effects, which can otherwise underestimate oxygen readings [23].

Background respiration including microbial oxygen demand should be accounted for by running parallel control cores without organisms. Subtracting these values from total oxygen consumption allows for the isolation of organismal respiration rates (faunal mediated oxygen consumption) [24]. This methodology not only allows for high-resolution tracking of physiological changes under EMF exposure but also helps link these individual-level responses to ecosystem-scale processes.

## CONCLUSIONS AND FUTURE WORK

A device for recreating magnetic fields typical for HVDC submarine cables was designed, constructed, and tested. The presented approach is an improvement over the setup consisting of Helmholtz coils, used in most publications, due to the inclusion of non-unform and non-unidirectional fields. The description of the setup, the testing, and the biological methods constitute a comprehensive guide that can be adopted in future biological experiments aiming to recreate conditions typical for HVDC cables. Future work will include the analysis of behaviour and physiology changes after exposure to magnetic fields typical for HVDC cables.

## ACKNOWLEDGMENTS

The authors would like to thank the National Grid Electricity Transmission for supporting the project and agreeing to the publication of results. Project Understanding the impact of Electromagnetic Fields from Interconnectors (BLUEFIN) (NIA2_NGET0057) was made possible through the Network Innovation Allowance.

This work was conducted under the Ecological Consequences of Offshore Wind (ECOWind) research programme (BOWIE project, grant NE/X008991/1, 2023-2027), funded by The Crown Estate's Offshore Wind Evidence and Change Programme (OWEC), The Crown Estate Scotland (CES) and by the Natural Environment Research Council (NERC) and supported by the

Department for Environment, Food and Rural Affairs (Defra).

## REFERENCES


[1] Z. L. Hutchison, A. B. Gill, P. Sigray, H. He, and J. W. King, 'Anthropogenic electromagnetic fields (EMF) influence the behaviour of bottom-dwelling marine species', *Sci Rep*, vol. 10, no. 1, p. 4219, 2020.

[2] S. J. England and D. Robert, 'The ecology of electricity and electroreception', *Biological Reviews*, vol. 97, no. 1, pp. 383–413, Feb. 2022.

[3] J. M. Anderson, T. M. Clegg, L. V. M. V. Q. Véras, and K. N. Holland, 'Insight into shark magnetic field perception from empirical observations', *Sci Rep*, vol. 7, no. 1, Dec. 2017.

[4] K. J. Lohmann and C. M. F. Lohmann, 'Detection of magnetic field intensity by sea turtles', *Nature*, vol. 380, no. 6569, pp. 59–61, 1996.

[5] L. C. Naisbett-Jones and K. J. Lohmann, 'Magnetoreception and magnetic navigation in fishes: a half century of discovery', Jan. 01, 2022, *Springer Science and Business Media Deutschland GmbH*.

[6] R. Bochert and M. L. Zettler, 'Long-term exposure of several marine benthic animals to static magnetic fields', *Bioelectromagnetics*, vol. 25, no. 7, pp. 498–502, 2004.

[7] K. Scott, P. Harsanyi, and A. R. Lyndon, 'Understanding the effects of electromagnetic field emissions from Marine Renewable Energy Devices (MREDs) on the commercially important edible crab, Cancer pagurus (L.)', *Mar Pollut Bull*, vol. 131, pp. 580–588, 2018.

[8] K. Scott, P. Harsanyi, B. A. A. Easton, A. J. R. Piper, C. M. V. Rochas, and A. R. Lyndon, 'Exposure to electromagnetic fields (Emf) from submarine power cables can trigger strength-dependent behavioural and physiological responses in edible crab, cancer pagurus (l.)', *J Mar Sci Eng*, vol. 9, no. 7, Jul. 2021.

[9] M. Jakubowska-Lehrmann, M. Białowąs, Z. Otremba, A. Hallmann, S. Śliwińska-Wilczewska, and B. Urban-Malinga, 'Do magnetic fields related to submarine power cables affect the functioning of a common bivalve?', *Mar Environ Res*, vol. 179, p. 105700, 2022.

[10] M. Jakubowska, M. Greszkiewicz, D. P. Fey, Z. Otremba, B. Urban-Malinga, and E. Andrulewicz, 'Effects of magnetic fields related to submarine power cables on the behaviour of larval rainbow trout (Oncorhynchus mykiss)', *Mar Freshw Res*, vol. 72, no. 8, pp. 1196–1207, Jul. 2021.

[11] D. P. Fey, M. Jakubowska, M. Greszkiewicz, E. Andrulewicz, Z. Otremba, and B. Urban-Malinga, 'Are magnetic and electromagnetic fields of anthropogenic origin potential threats to early life stages of fish?', *Aquatic Toxicology*, vol. 209, pp. 150–158, Apr. 2019.

[12] L. Albert, F. Olivier, A. Jolivet, L. Chauvaud, and S. Chauvaud, 'Effects of anthropogenic magnetic fields on the behavior of a major predator of the intertidal and subtidal zones, the velvet crab Necora puber', *Mar Environ Res*, vol. 190, Sep. 2023.

[13] P. Harsanyi *et al.*, 'The Effects of Anthropogenic Electromagnetic Fields (EMF) on the Early Development of Two Commercially Important Crustaceans, European Lobster, Homarus gammarus (L.) and Edible Crab, Cancer pagurus (L.)', *J Mar Sci Eng*, vol. 10, no. 5, May 2022.

[14] C. M. F. Durif *et al.*, 'Magnetic fields generated by submarine power cables have a negligible effect on the swimming behavior of Atlantic lumpfish (Cyclopterus lumpus) juveniles', *PeerJ*, vol. 11, Jan. 2023.

[15] E. C. N. Chapman, C. M. V Rochas, A. J. R. Piper, J. Vad, and G. Kazanidis, 'Effect of electromagnetic fields from renewable energy subsea power cables on righting reflex and physiological response of coastal invertebrates', *Mar Pollut Bull*, 2023.

[16] B. Taormina *et al.*, 'Impact of magnetic fields generated by AC/DC submarine power cables on the behavior of juvenile European lobster (Homarus gammarus)', *Aquatic Toxicology*, vol. 220, Mar. 2020.

[17] COMSOL Multiphysics, 'Magnetic Field of a Helmholtz Coil', https://www.comsol.com/model/magnetic-field-of-a-helmholtz-coil-15.

[18] Z. Huang, 'Rating methodology of high voltage mass impregnated DC cable circuits', University of Southampton, 2014.

[19] J. Rzempoluch *et al.*, 'Electric Fields Induced by Water Movement in Proximity to HVDC Submarine Cables', *IEEE Journal of Oceanic Engineering*, vol. 50, no. 3, pp. 2369–2380, 2025.

[20] M. Solan, B. J. Cardinale, A. L. Downing, K. A. M. Engelhardt, J. L. Ruesink, and D. S. Srivastava, 'Extinction and Ecosystem Function in the Marine Benthos', *Science (1979)*, vol. 306, no. 5699, pp. 1177–1180, Nov. 2004.

[21] C. M. Koretsky, C. Meile, and P. Van Cappellen, 'Quantifying bioirrigation using ecological parameters: a stochastic approach†', *Geochem Trans*, vol. 3, no. 1, p. 17, 2002.

[22] S. Forster, R. N. Glud, J. K. Gundersen, and M. Huettel, 'In situ Study of Bromide Tracer and Oxygen Flux in Coastal Sediments', *Estuar Coast Shelf Sci*, vol. 49, no. 6, pp. 813–827, 1999.

[23] G. G. Rodgers, P. Tenzing, and T. D. Clark, 'Experimental methods in aquatic respirometry: the importance of mixing devices and accounting for background respiration', *J Fish Biol*, vol. 88, no. 1, pp. 65–80, Jan. 2016.

[24] T. Sanders, M. Solan, and J. A. Godbold, 'Intraspecific variability across seasons and geographically distinct populations can modify species contributions to ecosystems', *Funct Ecol*, vol. 39, no. 3, pp. 698–710, Mar. 2025.


## GLOSSARY

**SCAMPI:** Synthetic Cable for the Assessment of Marine Power Impacts
**EMF**: Electromagnetic Field